Available online at www.sciencedirect.com

ScienceDirect

Advances in Climate Change Research 17 (2026) 338–346

www.keaipublishing.com/en/journals/accr/

Research

Daily imaging from China's HJ-2A/B satellites enables yearly mapping of regional glacial lakes

Yong NIE[a,*], Wen WANG[a,b], Hamish D. PRITCHARD[c], Chang-Jun GU[b,**], Qi-Yuan LYU[a], Yu-Hong WU[a,d], Su-Ju LI[b]

[a] *Key Laboratory of Mountain Hazards and Engineering Resilience, Institute of Mountain Hazards and Environment, Chinese Academy of Sciences, Chengdu 610213, China*

[b] *National Disaster Reduction Center of China, Ministry of Emergency Management, Beijing 100124, China*

[c] *British Antarctic Survey, Cambridge CB3 0ET, UK*

[d] *University of Chinese Academy of Sciences, Beijing 101408, China*

Received 12 July 2025; revised 29 September 2025; accepted 10 December 2025
Available online 18 December 2025

Abstract

The rapid expansion of glacial lakes in high-mountain regions, both in number and area, increases the risk of Glacial Lake Outburst Floods (GLOFs) to downstream communities. Optical remote sensing is essential for regional monitoring, as these lakes are frequently widespread and often inaccessible. However, clear image acquisition in mountainous areas is regularly hindered by shadowing, seasonal snow, and cloud cover. In the Himalayas, more frequent imaging is necessary to accurately inventory lakes during the short, snow-free periods. The HJ-2A/B satellites deployed by China now provide daily revisits at 16 m resolution, enabling comprehensive, high-quality mapping of glacial lakes. This study introduces a novel framework that uses a deep-learning U-Net model to detect lakes in HJ-2 imagery automatically and assesses its efficacy for monitoring lake changes in the China–Nepal section of the Central Himalayas (CNCH). Our findings indicate that the frequent imaging capabilities of HJ-2 permit annual lake mapping within a specific 1-mon period, achieving an accuracy and sensitivity to area changes exceeding 99%, with the ability to detect changes as small as 0.004 km^2. In our case study, we identify 2738 lakes in 2022 and 2739 lakes in 2023, with respective areas of 256.51 ± 14.41 km^2 and 260.89 ± 14.59 km^2. Despite certain limitations in geometric and radiometric calibration, this study establishes that HJ-2 imagery is highly effective for consistent, frequent monitoring of glacial lake changes and GLOF risks compared to previous satellite imagery.

Keywords: Remote sensing; Glacial lake outburst floods; Deep learning model; Central Himalayas

1. Introduction

As climate change increasingly affects mountain environments and their water resources (Li et al., 2022; Nie et al., 2021; Pritchard, 2019), satellite imaging becomes indispensable for observing environmental changes and the evolution of natural hazards in these regions (Chen et al., 2023; Wulder et al., 2019; Zhang et al., 2023a). Glacial lakes, for example, serve as a sensitive indicator of climate change and have expanded in the Himalayas over recent decades (Nie et al., 2017). Glacial lake outburst floods (GLOFs) have also increased in frequency, posing a growing threat to downstream populations and infrastructure (Nie et al., 2023). The Central Himalayan region is particularly vulnerable to GLOFs, which have led to catastrophic socio-economic losses in recent years (Nie et al., 2018), as exemplified by the Purepu GLOF in

* Corresponding author.
** Corresponding author.
E-mail addresses: nieyong@imde.ac.cn (NIE Y.), guchangjun@ndrcc.org.cn (GU C.-J.).

Peer review under responsibility of National Climate Centre (China Meteorological Administration)

https://doi.org/10.1016/j.accre.2025.12.006

Gyirong County on July 8, 2025. Glacial lakes in this region, however, are often widely distributed, remote, and difficult to monitor on the ground. Satellite remote sensing, therefore, provides the most practical approach for monitoring lake evolution and identifying GLOF hazards on a regional scale (Lesi et al., 2022; Nie et al., 2017; Zhang et al., 2024).

Many optical Earth Observation sensors, such as the Landsat series and Sentinel-2, have been launched and are commonly used for land use studies, glacial lake mapping, and monitoring disaster events (Gu et al., 2023; Lesi et al., 2022; Xiong et al., 2024) because they are readily available, have a relatively high resolution (10−30 m), and provide a cost-effective alternative to higher-resolution commercial satellite images (Wulder et al., 2019). However, optical imaging in mountain regions is often hindered by clouds, cloud shadows, steep terrain, and seasonal snow cover, resulting in gaps in the observational record (Lesi et al., 2022; Wieland et al., 2022; Wright et al., 2024). While images from different years have been utilized to create regional inventories of glacial lakes (Wang et al., 2020; Zhang et al., 2015, 2023b), the challenge of frequently mapping lake evolution remains due to these observation gaps.

Shorter revisit times play a crucial role in enhancing the monitoring capacity of satellite observations of surface change by increasing the likelihood of acquiring useable images of the Earth's surface. Combining data from Landsat 8 and Landsat 9 (Wulder et al., 2019), the original revisit period of 16 d can be reduced to 8 d, while a combination of Sentinel-2 A and B reduces this to 5 d (Li et al., 2024). The advantage of a shorter revisit period is evident in annual composite images produced by Google Earth Engine from the Landsat 8, Landsat 9, combined Landsat 8−9, and Sentinel-2 datasets. Within a 10 km buffer zone of glaciers (RGI Consortium, 2017) in the China−Nepal section of the Central Himalayas (CNCH), the extent of 'void pixels,' where the surface is obscured year-round, ranges from 8% to 14% in the Landsat-based analysis for 2022 and 2023, compared to only ~1% for Sentinel-2 in 2022 (Figs. A1−A2 and Table A1). Despite these shorter observation intervals, void pixels and their concentration near glacial lakes hinder frequent mapping of these lakes with Landsat/Sentinel, making hazard detection less reliable or, at times, impossible.

In late 2020, the HJ-2 A and B satellites were successfully launched, offering five visible bands with a spatial resolution of 16 m and a swath width of 800 km (Li et al., 2024). Notably, the HJ-2 satellite constellation, which succeeds HJ-1 (Zhang et al., 2023a), revisits the same location within just 1 d. HJ-2 imagery finds use in flood mapping research and lake water quality monitoring (Gu et al., 2023; Li et al., 2024; Wang et al., 2024), but HJ-2 images rarely appear in studies related to glacial lakes, leaving their potential for regional-scale mapping and annual monitoring of alpine glacial lakes largely unexplored.

In this study, we evaluate the suitability of rapid-revisit observations from the HJ-2A/B satellites for automatically extracting alpine glacial lake boundaries, thereby facilitating the annual monitoring of regional glacial lake dynamics. We develop a glacial lake mapping method using a deep learning model to identify lake boundaries from HJ-2 images, and we demonstrate this analysis by repeatedly mapping the glacial lakes of the entire CNCH region for 2022 and 2023. Finally, we explore the capabilities and limitations of HJ-2 images in glacial lake research. This study highlights HJ-2's daily imagery as a crucial resource for developing consistent annual glacial lake inventories, thereby filling data gaps in high-altitude cryosphere studies. It enhances GLOF risk evaluations in regions such as the Himalayas and facilitates assessing the effects of climate change on glacial lakes.

2. Materials and methods

2.1. Study area

We defined the study area by dividing the Central Himalayas using the Nepali border and the corresponding connected main ranges in the Chinese section. Our CNCH study area (Fig. 1) spans 22,000 km^2 and contains 5743 glaciers (covering 6391 km^2) that have lost mass over the past few decades (Nie et al., 2021; RGI Consortium, 2017). With socio-economic development, the CNCH becomes an increasingly important corridor for China−Nepal trade. Still, it faces threats from glacial retreat, the expansion of glacial lakes, and the rising risk of GLOFs, which endanger local communities, transportation, and expanding hydropower infrastructure (Nie et al., 2017; Zheng et al., 2021). Since 1981, the CNCH has experienced 18 recorded GLOF events, some of which, such as the Cirenmaco GLOF in 1981, the Gongbashatong Tsho GLOF in 2016, and the Purepu GLOF in 2025, cause catastrophic damage (Nie et al., 2018).

2.2. Data

We use a total of 87 images from satellites HJ-2A and HJ-2B to create a glacial lake dataset for 2022 and 2023, of which 12 are employed to train the deep-learning model (Fig. 2). The advantages of HJ-2 data include a daily revisit capability, 16 m spatial resolution, and an 800 km swath width (Gu et al., 2023), giving users more options for monitoring land surface changes compared to Landsat and Sentinel-2 imagery (Li et al., 2024). The overlap frequency of our HJ-2 images exceeds 5 images for most of the study area and 10 for around half of the alpine regions where glacial lakes are distributed. This high overlap rate helps mitigate the impacts of clouds, snow, and topographic shading on glacial lake mapping (see also Section 3.3).

All HJ-2 images from https://data.cresda.cn/were captured during the post-monsoon period in October 2022 and 2023, with 63% of the imagery acquired in late October.

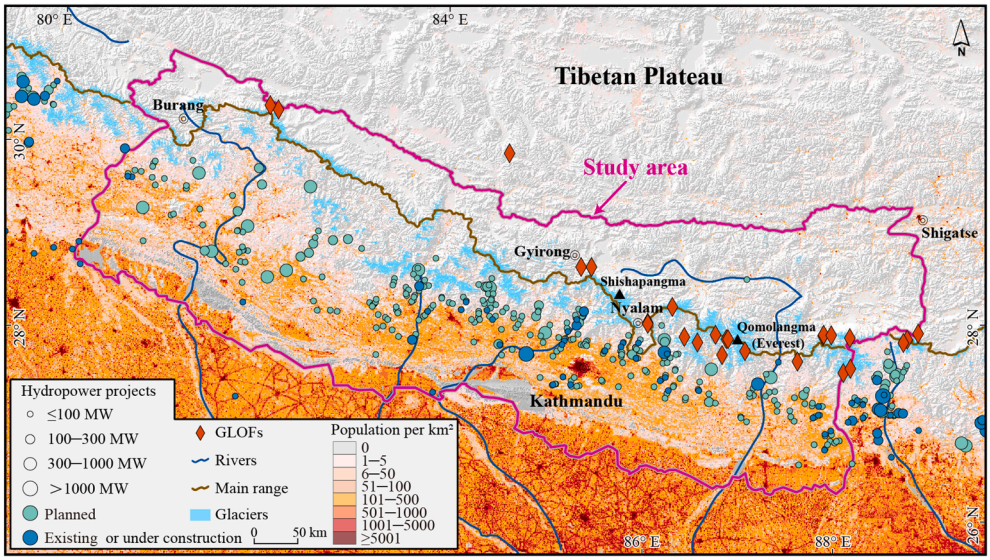

Fig. 1. Location of the study area and distribution of recorded GLOFs (Nie et al., 2023), hydropower projects (HPPs) (Nie et al., 2021), and glaciers.

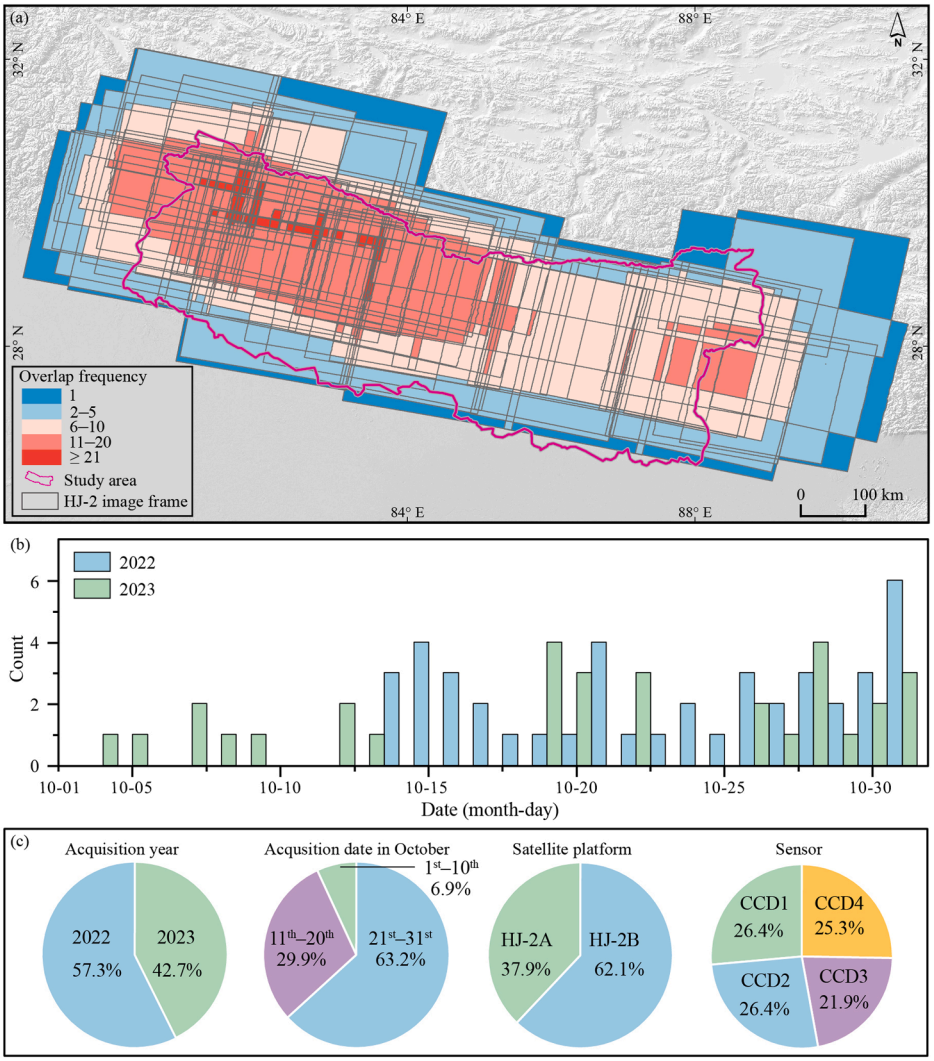

Fig. 2. The frequency of spatial overlap and the acquisition dates of the HJ-2 images (a–b) in October 2022 and 2023, and the proportion of HJ-2 images used based on the acquisition year, date, satellite platform, and sensors (c).

The number of images from 2022 is 15% higher than in 2023, while the HJ-2B satellite provided 24% more images than the HJ-2A platform. Each HJ-2 imaging sensor (Charge-Coupled Device, CCD) generates nearly equal amounts of data for the study area and spans the spectral red-edge band, plus similar spectral intervals for the near-infrared, red, green, and blue bands (Li et al., 2024) as the Sentinel-2 multispectral imager (MSI) and Landsat-8/9 operational land imager (OLI).

To aid our analysis, we use the Shuttle Radar Topography Mission Digital Elevation Model (SRTM DEM) to model topographic shading in our images (USGS, 2015). We define a 10 km buffer zone around the glaciers of the Randolph Glacier Inventory (RGI) 6.0 (RGI Consortium, 2017) to assist in distinguishing glacial and non-glacial lakes and to categorize glacial lakes into 'supraglacial', 'ice-contact', and 'ice-unconnected' types. We also use high-resolution imagery from Google Earth (© Google Earth, 2019) to manually digitize glacial lake boundaries as a reference for validating our automated HJ-2-derived lake mapping. We employed 64 Landsat and 58 Sentinel-2 images between 2022 and 2023 to extract validation samples for comparison with the HJ-2-derived result.

2.3. Methods

We develop a new framework to map glacial lakes using HJ-2 images (Fig. 3). The workflow consists of four stages: 1) data preprocessing, 2) mask creation, 3) model training, and 4) glacial lake mapping and postprocessing.

In stage 1, we stack all five bands of the HJ-2 images that record reflectance at the top of the atmosphere (TOA). These images are provided by the Key Laboratory of Emergency Satellite Engineering and Application, Ministry of Emergency Management. We received high-quality HJ-2 images acquired between 2020 and 2023, which had already undergone geometric and radiometric calibration. After a thorough comparison and analysis, we exclude images from 2020 to 2021 due to inaccuracies in the geometric rectification process.

In stage 2, we create a cloud mask using the UKIS-CSMASK algorithm (Wieland et al., 2022). We generate a topographic-shadow mask (Burrough and McDonnell, 1998) using the SRTM DEM and the solar azimuth and zenith angles at the time of imaging, with a shadow threshold of <128 (Fig. A3).

In stage 3, we train a U-Net model for semantic segmentation to predict the boundaries of glacial lakes

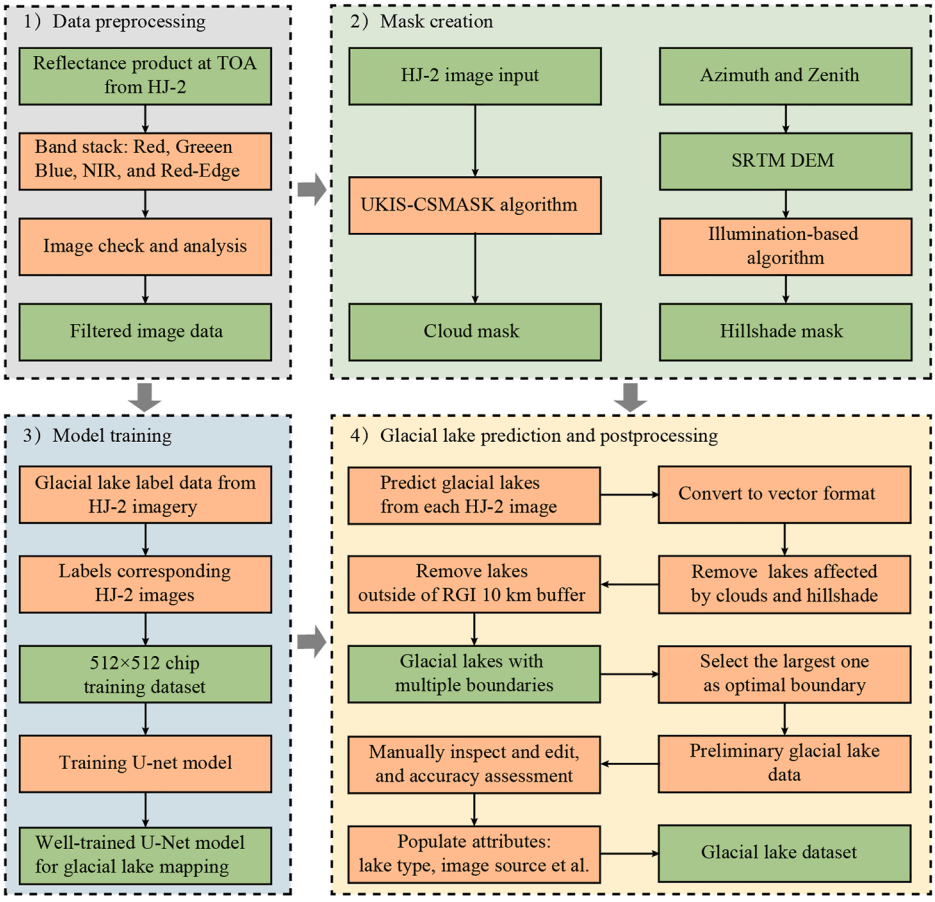

Fig. 3. The workflow for mapping glacial lakes using HJ-2 imagery (The orange box indicates a processing step, while the green box shows input and output data).

(Ronneberger et al., 2015), following a comparison of various machine learning models. As a top-performing deep learning model for image segmentation (Azad et al., 2024; Ronneberger et al., 2015), U-Net is effective at identifying water bodies and has been successfully employed for mapping lakes and reservoirs (Li et al., 2025; Pi et al., 2022; Zhang et al., 2026). Using a semi-automated lake mapping method (Lesi et al., 2022), we generate labeled data for 7683 glacial lakes to train the model using 12 HJ-2 images. We split the labels and images into 24,364 samples of 512 × 512 pixel tiles, which we randomly divide into training, validation, and test sets at 8:1:1. The hyperparameters for the U-Net model include 200 epochs, the Adam optimizer, an initial learning rate of 0.0001, a batch size of 32, and a stepwise learning rate decay schedule. The trained model achieves satisfactory accuracy metrics, including 87% precision, 92% recall, 89% F1-score, and 81% Intersection over Union (IoU). We subsequently use this model setup to map glacial lakes from the full set of HJ-2 images.

In stage 4, we convert the glacial lakes extracted by our well-trained model from raster to vector format for each image and exclude those lakes that were overlapped by our cloud or shadow masks by more than 5%. Additionally, we exclude lakes located outside the 10 km buffer zone from any glacier (Wang et al., 2020; Zheng et al., 2021). When the same glacial lake is repeatedly mapped with multiple boundaries, we automatically select the largest boundary as the optimal one. We apply a minimum mapping unit (MMU) of 2560 m^2 to exclude lakes smaller than this threshold, and we rigorously inspect the resulting preliminary glacial lake dataset across the study area, correcting any errors identified during manual inspection. We randomly selected 129 lakes for a detailed accuracy assessment against manually digitized areas of these lakes using independent, high-resolution Google Earth images of similar age (given the lack of in-situ field investigations in the study area) (Fig. A4).

Finally, we record essential parameters of the glacial lakes, including area, perimeter, mapping uncertainty, elevation, image source, and type. All lakes are classified into three categories (Lesi et al., 2022)—supraglacial, ice-contact, and ice-unconnected—based on their spatial relationship with glaciers. This classification enables us to develop detailed datasets of glacial lakes for 2022 and 2023, using HJ-2 images for the CNCH study area. We estimate the mapping uncertainty using an improved Hanshaw and Bookhagen equation (after Lesi et al. (2022)), assuming a displacement error of half a pixel.

3. Results and discussion

3.1. Validation of the glacial lake data

Our workflow applied to HJ-2 imagery effectively extracts glacial lake boundaries, achieving accuracy comparable to that of Landsat and Sentinel-2 imagery (Fig. A5 and Table A2). For the sample of 129 lake areas tested against manual digitization, most samples (118 out of 129) fall within a 95% confidence interval (Fig. A6). The size range (0.006–4.988 km^2, with a median and standard deviation of 0.051 ± 0.457 km^2) closely matches that of the digitized areas (0.008–4.953 km^2, with a median and standard deviation of 0.052 ± 0.459 km^2). The mean error of the individual HJ-2-derived lake area compared to the reference is 0.001 km^2 for 2023. The total discrepancy between HJ-2-derived lake areas and our manually digitized areas is 0.19 km^2 and 0.02 km^2 for 2022 and 2023, respectively, with area biases of 0.99% and 0.10%, respectively (Fig. A7 and Table A2).

3.2. Glacial lake distribution and change

Over the entire CNCH region, we mapped 2738 glacial lakes in 2022, covering an area of 256.51 ± 14.41 km^2, and 2739 glacial lakes covering an area of 260.89 ± 14.59 km^2 in 2023. These lakes are heterogeneous in spatial distribution, size, and type (Fig. 4). Larger glacial lakes are less frequent than smaller lakes but accounted for a larger fraction of the total area: lakes of the ≤0.02 km^2 class comprised nearly half the total number but accounted for the smallest fraction of the area (Fig. 5). Conversely, lakes in the >1.0 km^2 class are least frequent but occupy the largest fraction of the total area. By type, ice-unconnected glacial lakes dominate in both number and area (2365 lakes covering 160.39 ± 11.07 km^2 in 2023), followed by ice-contact and supraglacial lakes (Table A3). Geographically, glacial lakes are unevenly distributed between the China and Nepal sections of the CNCH (Fig. A8, Table A4). Specifically, in 2023, the Nepal section had 1230 glacial lakes covering approximately half the area of the 1509 glacial lakes in the China section (82.43 ± 5.74 km^2 versus 178.46 ± 8.85 km^2), with an average lake area that was also greater (0.12 km^2 versus 0.07 km^2).

A net increase in total lake number from 2738 to 2739 between 2022 and 2023 (Table A3) is dominated by a rise from 355 to 372 lakes in the mid-size category of 0.1–0.5 km^2 (Fig. 5). Our one-year interval between study epochs is too short to yield statistically significant area changes in most cases, but we note that the sign of the change (an increase in area) is consistent across all lake types (Table A3), in both Nepal and China sections (Table A4), and in the majority of size classes (Fig. 5). Over the full CNCH, our mapped lake area for 2022 is 256.51 ± 14.41 km^2, and for 2023 it is 260.89 ± 14.59 km^2. The statistics for the 0.1–0.5 km^2 lake category are 74.95 ± 3.91 km^2 and 77.08 ± 4.03 km^2, respectively. Lakes greater than 1.0 km^2 occupy the largest total area of 87.99 ± 1.71 km^2 in 2022 and 89.32 ± 1.78 km^2 in 2023. Supraglacial lakes, covering a relatively small total area, exhibit a high apparent growth rate of over 8% (from 4.93 ± 0.46 km^2 to 5.33 ± 0.47 km^2). A year-to-year spread of glacial lakes is indicated by the slight increase in number (Table A3) and is supported by the positive sign of these

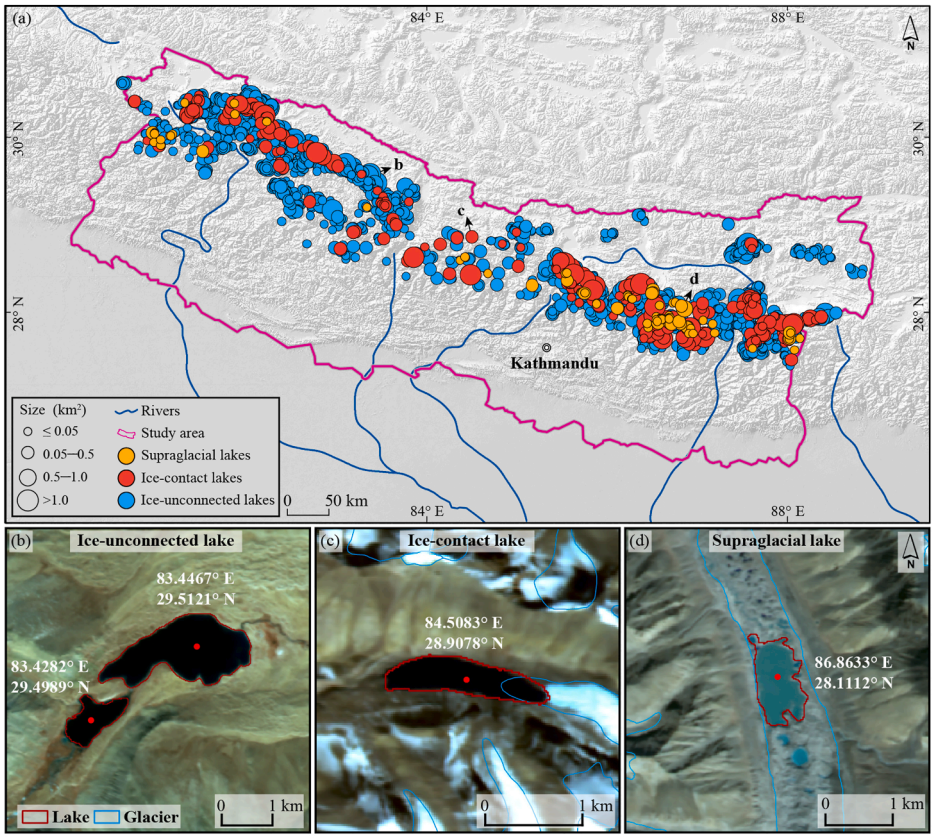

Fig. 4. Distribution of glacial lakes in the study area for 2023 (a) and examples of each type of glacial lake (red polygons in b–d) (Blue polygons show glacier margins as defined by RGI 6.0).

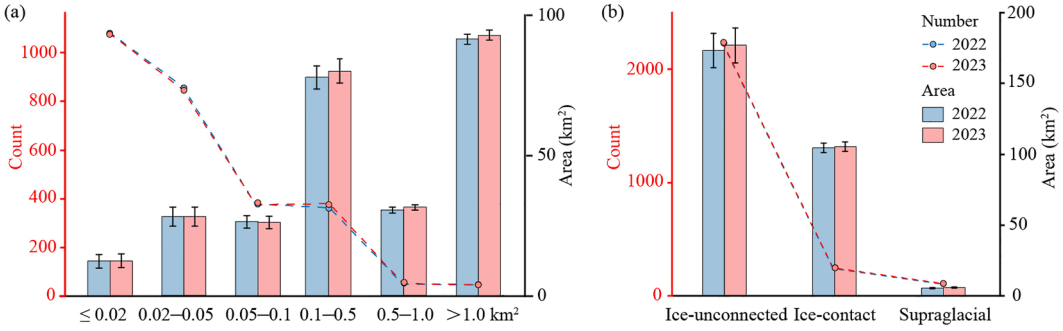

Fig. 5. Count (dots) and area (bars) of glacial lakes categorized by size groups (a) and types (b) for 2022 and 2023.

area statistics, which is consistent across multiple categories.

3.3. Advantages and limitations of HJ-2 images in glacial lake mapping

The HJ-2 satellite constellation, combined with our workflow, offers several advantages for high-frequency monitoring of glacial lakes at a regional scale. Specifically, the daily revisit capability, a swath width of 800 km, and a relatively high spatial resolution of 16 m (Gu et al., 2023; Li et al., 2024) enable lakes to be mapped accurately and repeatedly within a single season. The frequent revisit rate (eight times that of Landsat 8 or 9 imagery and five times that of Sentinel-2) enhances the availability of high-quality images, helping mitigate the effects of clouds and hill shading that would otherwise hinder glacial lake mapping. This high revisit frequency results in part from the degree of image overlap that is possible with the 800 km swath width (enabled by four CCDs on each HJ-2 satellite (Gu et al., 2023)), in contrast to the narrower swaths of Landsat and Sentinel-2 imagery (185 km and 290 km, respectively (Li et al., 2024)). These frequent revisits enable us to map all CNCH glacial lakes in the same calendar month (October) across consecutive years, thereby minimizing the impact of seasonal variations on inter-annual analyses. For

individual high-risk glacial lakes with infrequent cloud cover, frequent revisits of HJ-2 imagery often help analyze their monthly or seasonal changes, providing the latest status of glacial lakes for GLOF early warning assessment. Furthermore, HJ-2 satellites with nearly daily observation capabilities, combined with our proposed mapping framework, help detect recent GLOFs.

Compared with Landsat, HJ-2's fine spatial resolution also enables the detection of smaller glacial lakes and the mapping of lake areas with higher precision. For our 129 validation lakes, for example, the total mapping uncertainty is approximately 0.9 km^2 (~5%) for HJ-2 and around 1.7 km^2 (~9%) for Landsat 8 and 9 (Table A5). Sentinel-2 achieves a higher accuracy of approximately 0.6 km^2 (~4%), which, in principle, allows for the detection of smaller lake changes over time. However, the substantially higher revisit rate of HJ-2 remains an essential attribute of this system in detecting potentially dangerous lake trends.

Given the magnitude and uncertainty in lake-area change from 2022 to 2023 that we map using HJ-2 data, two to three years of sustained change are required for statistically significant regional-area trends to emerge. However, a change as small as 0.04 km^2 (around 3.5 football pitches) in the area of an individual lake could be detected in as little as one year (Table A5), demonstrating the value of this approach for early warning of lake growth associated with increased GLOF risk.

Despite these advantages, we identify some limitations in HJ-2 data (Fig. 6).

(1) Geometric distortion in HJ-2 images before 2022 makes them unusable for glacial lake mapping. Regulatory adjustments made on orbit during 2020–2021 caused distortions that could not be accurately orthorectified. Hence, the planned lake mapping for these years is not possible.
(2) The HJ-2 CCDs may require further radiometric calibration. While our mapping model performs well for most glacial lakes, some are inaccurately delineated due to issues with radiometric calibration (Fig. 6). This is indicated by the relatively poor

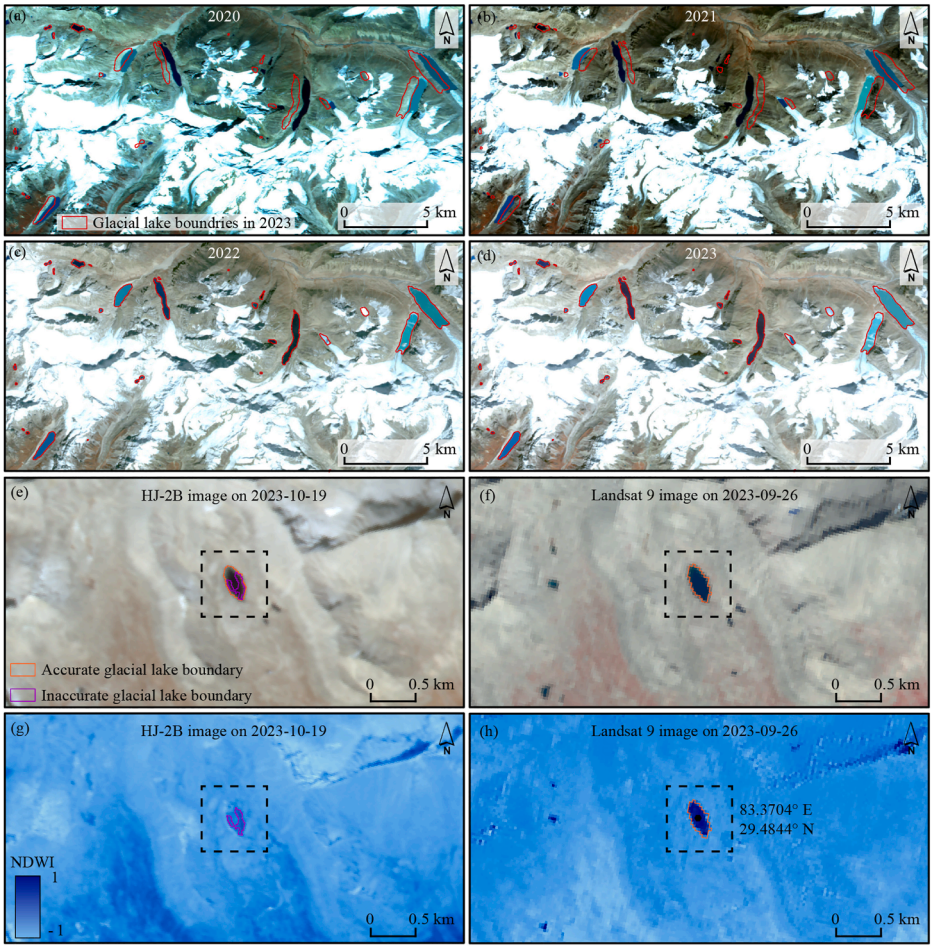

Fig. 6. Geometric distortion resulted in spatial mismatches between lake locations in HJ-2 images from 2020 to 2021 (a–b), compared to accurately rectified images from 2022 to 2023 (c–d), Radiometric issues with HJ-2 are suggested in this comparison of the same glacial lake imaged by HJ-2 and Landsat 9 (e–f), where HJ-2 exhibits a relatively weak and discontinuous NDWI lake signature that caused an incomplete boundary relative to Landsat 9 (g–h).

detectability of some lakes when using the Normalized Difference Water Index (NDWI) with HJ-2 data, in contrast to good detectability using the same algorithm with Landsat data (Fig. 6g−h).

(3) As is common with optical remote sensing methods, snow and cloud cover often restrict useable data collection in mountainous regions (Lesi et al., 2022; Wieland et al., 2022; Wright et al., 2024). As a result, monitoring glacial lake dynamics using HJ-2 images remains challenging during the Himalayan winter (December to May) and the summer monsoon (June to September) (Nie et al., 2017). Based on archival data comparisons, October is the optimal month for acquiring high-quality HJ-2 images in the CNCH. While inter-annual changes in glacial lakes can be analyzed in October using HJ-2 images, monitoring changes during other months remains unfeasible.

4. Conclusions

HJ-2 images offer a distinct advantage over Landsat and Sentinel-2 images for glacial lake mapping due to their greater revisit frequency. Inaccurate geometric rectification prevents the use of earlier HJ-2 images from 2020 to 2021. Radiometric limitations somewhat hinder the automated mapping of glacial lakes. Still, our case study in the CNCH demonstrates that HJ-2 images can be successfully used for automated mapping of glacial lakes and for monitoring changes in these lakes at high temporal resolution, supporting the potential to detect GLOFs. By increasing the number of image pixels free of clouds, snow, and shadows over observation periods within a one-month time window, HJ-2 analysis enables interannual monitoring of glacial lake changes at the regional scale. This capability is essential for climate change research, providing consistent, high-frequency data to monitor cryospheric changes, validate glacier water models, and evaluate GLOF risks from rapid ice loss. The HJ-2 satellite constellation plays a key role in observing climate impacts in high-mountain regions.

Declaration of competing interest

The authors declare no conflict of interest.

CRediT authorship contribution statement

Yong Nie: Writing − review & editing, Writing − original draft, Validation, Methodology, Funding acquisition, Conceptualization. **Wen Wang:** Writing − review & editing, Data curation. **Hamish D. Pritchard:** Writing − review & editing, Conceptualization. **Chang-Jun Gu:** Writing − original draft, Supervision, Resources, Project administration, Methodology, Conceptualization. **Qi-Yuan Lyu:** Writing − review & editing, Validation, Software. **Yu-Hong Wu:** Writing − review & editing, Visualization, Data curation. **Su-Ju Li:** Writing − review & editing, Resources, Project administration.

Acknowledgments

This work is funded by the National Natural Science Foundation of China (42171086), the National Key Research and Development Program of China (2022YFF0711704, 2021YFB3901205), the Science and Technology Department of Tibet Program (XZ202301ZY0016G), the Key Laboratory of Emergency Satellite Engineering and Application, Ministry of Emergency Management, and the Key Laboratory of Mountain Hazards and Engineering Resilience, Chinese Academy of Sciences (Grant number KLMHER-T09).

Appendix A. Supplementary data

Supplementary data to this article can be found online at https://doi.org/10.1016/j.accre.2025.12.006.

References

Azad, R., Aghdam, E.K., Rauland, A., et al., 2024. Medical image segmentation review: the success of U-NET. IEEE Trans. Pattern Anal. Mach. Intell. 46 (12), 10076−10095.

Burrough, P.A., Mcdonnell, R.A., 1998. Principles of Geographic Information Systems. Oxford University Press, New York.

Chen, F., Zhao, H., Roberts, D., et al., 2023. Mapping center pivot irrigation systems in global arid regions using instance segmentation and analyzing their spatial relationship with freshwater resources. Remote Sens. Environ. 297, 113760.

Gu, C., Li, S., Liu, M., et al., 2023. Monitoring glacier lake outburst flood (GLOF) of Lake Merzbacher using dense Chinese high-resolution satellite images. Remote Sens. 15 (7), 1941.

Lesi, M., Nie, Y., Shugar, D.H., et al., 2022. Landsat- and Sentinel-derived glacial lake dataset in the China−Pakistan economic corridor from 1990 to 2020. Earth Syst. Sci. Data 14 (12), 5489−5512.

Li, D., Lu, X., Walling, D.E., et al., 2022. High Mountain Asia hydropower systems threatened by climate-driven landscape instability. Nat. Geosci. 15 (7), 520−530.

Li, J., Li, Y., Yu, Y., et al., 2024. Evaluating the capabilities of China's new satellite HJ-2 for monitoring chlorophyll a concentration in eutrophic lakes. Int. J. Appl. Earth Obs. Geoinf. 126, 103618.

Li, L., Long, D., Wang, Y., et al., 2025. Global dominance of seasonality in shaping lake-surface-extent dynamics. Nature 642 (8067), 361−368.

Nie, Y., Deng, Q., Pritchard, H.D., et al., 2023. Glacial lake outburst floods threaten Asia's infrastructure. Sci. Bull. 68 (13), 1361−1365.

Nie, Y., Liu, Q., Wang, J., et al., 2018. An inventory of historical glacial lake outburst floods in the Himalayas based on remote sensing observations and geomorphological analysis. Geomorphology 308, 91−106.

Nie, Y., Pritchard, H.D., Liu, Q., et al., 2021. Glacial change and hydrological implications in the Himalaya and Karakoram. Nat. Rev. Earth Environ. 2 (2), 91−106.

Nie, Y., Sheng, Y., Liu, Q., et al., 2017. A regional-scale assessment of Himalayan glacial lake changes using satellite observations from 1990 to 2015. Remote Sens. Environ. 189 (2), 1−13.

Pi, X., Luo, Q., Feng, L., et al., 2022. Mapping global lake dynamics reveals the emerging roles of small lakes. Nat. Commun. 13 (1), 5777.

Pritchard, H.D., 2019. Asia's shrinking glaciers protect large populations from drought stress. Nature 569 (7758), 649−654.

RGI Consortium, 2017. Randolph Glacier Inventory: A Dataset of Global Glacier Outlines, Version 6. National Snow and Ice Data Center, Boulder, Colorado USA.

Ronneberger, O., Fischer, P., Brox, T., 2015. U-Net: Convolutional Networks for Biomedical Image Segmentation. In: Navab, N.,

Hornegger, J., Wells, W.M. (Eds.), et al., Medical Image Computing and Computer-Assisted Intervention − MICCAI 2015. Springer International Publishing, Cham, pp. 234−241.

USGS, 2015. The Shuttle Radar Topography Mission (SRTM) Collection User Guide at. https://lpdaac.usgs.gov/documents/179/SRTM_User_Guide_V3.pdf. (Accessed 10 June 2019).

Wang, X., Guo, X., Yang, C., et al., 2020. Glacial lake inventory of high-mountain Asia in 1990 and 2018 derived from landsat images. Earth Syst. Sci. Data 12 (3), 2169−2182.

Wang, Z., Wang, X., Li, G., et al., 2024. Historical information fusion of dense multi-source satellite image time series for flood extent mapping. Inf. Fusion 109, 102445.

Wieland, M., Fichtner, F., Martinis, S., 2022. UKIS-CSMASK: a python package for multi-sensor cloud and cloud shadow segmentation. The international archives of the photogrammetry. Remote Sens. Spat. Inform. Sci. XLIII-B3-2022 217−222.

Wright, N., Duncan, J.M.A., Callow, J.N., et al., 2024. CloudS2Mask: a novel deep learning approach for improved cloud and cloud shadow masking in Sentinel-2 imagery. Remote Sens. Environ. 306, 114122.

Wulder, M.A., Loveland, T.R., Roy, D.P., et al., 2019. Current status of landsat program, science, and applications. Remote Sens. Environ. 225, 127−147.

Xiong, S., Zhang, X., Lei, Y., et al., 2024. Time-series China urban land use mapping (2016−2022): an approach for achieving spatial-consistency and semantic-transition rationality in temporal domain. Remote Sens. Environ. 312, 114344.

Zhang, G., Bolch, T., Yao, T., et al., 2023b. Underestimated mass loss from lake-terminating glaciers in the greater Himalaya. Nat. Geosci. 16 (4), 333−338.

Zhang, G., Yao, T., Xie, H., et al., 2015. An inventory of glacial lakes in the Third Pole region and their changes in response to global warming. Global Planet. Change 131, 148−157.

Zhang, H., Nie, Y., Liu, L., et al., 2026. An advanced deep learning framework for mapping glacial lakes and its application in the Hindu Kush−Karakoram−Himalaya region. J. Hydrol. 664, 134507.

Zhang, S., Nie, Y., Zhang, H., 2024. Glacial lake changes and risk assessment in Rongxer watershed of China−Nepal economic corridor. Remote Sens. 16 (4), 725.

Zhang, Z., Lu, L., Zhao, Y., et al., 2023a. Recent advances in using Chinese Earth observation satellites for remote sensing of vegetation. ISPRS-J. Photogramm. Remote Sens. 195, 393−407.

Zheng, G., Allen, S.K., Bao, A., et al., 2021. Increasing risk of glacial lake outburst floods from future Third Pole deglaciation. Nat. Clim. Change 11 (5), 411−417.